scientific reports

Check for updates

OPEN

Electrostatic regulation of the *cis*- and *trans*-membrane interactions of synaptotagmin-1

Houda Yasmine Ali Moussa[1] & Yongsoo Park[1,2]✉

Synaptotagmin-1 is a vesicular protein and Ca^{2+} sensor for Ca^{2+}-dependent exocytosis. Ca^{2+} induces synaptotagmin-1 binding to its own vesicle membrane, called the *cis*-interaction, thus preventing the *trans*-interaction of synaptotagmin-1 to the plasma membrane. However, the electrostatic regulation of the *cis*- and *trans*-membrane interaction of synaptotagmin-1 was poorly understood in different Ca^{2+}-buffering conditions. Here we provide an assay to monitor the *cis*- and *trans*-membrane interactions of synaptotagmin-1 by using native purified vesicles and the plasma membrane-mimicking liposomes (PM-liposomes). Both ATP and EGTA similarly reverse the *cis*-membrane interaction of synaptotagmin-1 in free [Ca^{2+}] of 10–100 μM. High PIP_2 concentrations in the PM-liposomes reduce the Hill coefficient of vesicle fusion and synaptotagmin-1 membrane binding; this observation suggests that local PIP_2 concentrations control the Ca^{2+}-cooperativity of synaptotagmin-1. Our data provide evidence that Ca^{2+} chelators, including EGTA and polyphosphate anions such as ATP, ADP, and AMP, electrostatically reverse the *cis*-interaction of synaptotagmin-1.

Exocytosis is the process of vesicle fusion and neurotransmitter release regulated by soluble *N*-ethylmaleimide-sensitive factor attachment protein receptor (SNARE) proteins, which are currently considered to be the catalysts of the fusion reaction[1,2]. Neuronal SNARE proteins are selectively expressed in neurons and neuroendocrine cells, and regulate release of neurotransmitters and hormones[3]. Neuronal SNARE proteins consist of syntaxin-1 and SNAP-25 in the plasma membrane, and vesicle-associated membrane protein-2 (VAMP-2) (also called synaptobrevin-2) in the vesicle membrane[1]. Synaptotagmin-1 is a Ca^{2+} sensor for fast Ca^{2+}-dependent exocytosis as an electrostatic switch[4]. The C2AB domain of synaptotagmin-1 coordinates Ca^{2+} binding, and the Ca^{2+}-bound C2AB domain penetrates negatively-charged anionic phospholipids by electrostatic interaction[2]. Several different models of synaptotagmin-1 to describe the process of Ca^{2+}-dependent vesicle fusion have been proposed, but the molecular mechanisms of synaptotagmin-1 remain controvertial[5].

Synaptotagmin-1 is a vesicular protein and interacts with anionic phospholipids electrostatically[5]. Native vesicles contain ~ 15% anionic phospholipids including phosphatidylserine (PS) and phosphatidylinositol (PI)[6], so Ca^{2+} induces synaptotagmin-1 binding to its own vesicle membrane, i.e., the *cis*-interaction[7,8]. Ca^{2+} fails and even slightly reduces vesicle fusion in the in-vitro reconstitution system, because synaptotagmin-1 preferentially interacts with vesicle membranes due to the physical proximity and this *cis*-membrane interaction prevents the *trans*-interaction of synaptotagmin-1 with the target membranes[7–9]. We have reported that ATP reverses this inactivating *cis*-interaction of synaptotagmin-1 by the electrostatic effect, and the *trans*-membrane interaction of synaptotagmin-1 only occurs to trigger vesicle fusion in-vivo[10]. This ATP effect on the *cis*-membrane interaction of synaptotagmin-1 has been confirmed independently: in a vesicle sedimentation assay a few hundred μM ATP electrostatically prevents a *cis*-configuration of synaptotagmin-1[11], and in a fusion assay using a colloidal probe microscopy and pore-spanning membranes ATP accelerates full fusion by preventing the *cis*-interaction without affecting the trans-interaction of synaptotagmin-1[12]. However, the electrostatic regulation of the *cis*- and *trans*-membrane interaction of synaptotagmin-1 to trigger Ca^{2+}-dependent vesicle fusion has not been described in detail.

Although synaptotagmin-1 is a conserved Ca^{2+} sensor for synchronous release of diverse vesicles including synaptic vesicles, large dense-core vesicles (LDCVs), and other secretory granules, the mechanism by which Ca^{2+}-cooperativity is regulated is not clear. The Hill coefficient (n) in the Ca^{2+} dose–response curves for exocytosis represents Ca^{2+}-cooperativity and the Hill coefficient varies depending on cell types from 2 to 5; e.g. calyx-of-Held synapses (n, 4.2)[13–15], neuromuscular junctions (n, 3.8)[16], bipolar cells (n, 4)[17], pituitary melanotrophs (n,

[1]Neurological Disorders Research Center, Qatar Biomedical Research Institute (QBRI), Hamad Bin Khalifa University (HBKU), Qatar Foundation, Doha, Qatar. [2]College of Health and Life Sciences (CHLS), Hamad Bin Khalifa University (HBKU), Qatar Foundation, Doha, Qatar. ✉email: ypark@hbku.edu.qa

2.5)[18], and chromaffin cells (n, 1.8)[19]. The Hill coefficient is the intrinsic property of each cell type and factors that regulate Ca^{2+}-cooperativity are poorly understood.

Synaptotagmin-1 binds to anionic phospholipids by electrostatic interaction and the Ca^{2+}-binding loops of the C2 domains penetrate anionic phospholipids by reducing repulsion between anionic phospholipids and acidic residues in the C2AB domain[4]. The polybasic patch in the C2B domain electrostatically interacts with PIP_2 in a Ca^{2+}-independent manner[20], and thereby increases the Ca^{2+}-sensitivity of synaptotagmin-1 membrane binding[10,21]. Given that the C2AB domain has five possible Ca^{2+}-binding sites[22,23] and therefore may have the Hill coefficient up to 4–5, but whether local PIP_2 concentrations regulate Ca^{2+}-cooperativity is not known.

Here we provide an assay to monitor the *cis*- and *trans*-membrane interaction of synaptotagmin-1 by using native LDCVs and the plasma membrane-mimicking liposomes (PM-liposomes). Ca^{2+} chelators, including EGTA and polyphosphate anions such as ATP, ADP, and AMP, electrostatically reverse the *cis*-interaction of synaptotagmin-1. Both ATP and EGTA, as Ca^{2+} chelators, have a similar effect to prevent the *cis*-membrane interaction of synaptotagmin-1 in free [Ca^{2+}] of 10–100 µM, but ATP, which has a good buffering capacity in the range of 10–500 µM free [Ca^{2+}], is an excellent Ca^{2+} buffer to study vesicle fusion and synaptotagmin-1 membrane binding. When the *trans*-membrane interaction of synaptotagmin-1 only occurs, high PIP_2 concentrations in the PM-liposomes decrease the Hill coefficient of vesicle fusion and synaptotagmin-1 membrane binding to ~ 2, suggesting that local PIP_2 concentrations might control Ca^{2+}-cooperativity of synaptotagmin-1.

Material and methods

Purification of large dense-core vesicles (LDCVs). LDCVs, also known as chromaffin granules, were purified from bovine adrenal medullae by using continuous sucrose gradient, then resuspended in a solution of 120 mM K-glutamate, 20 mM K-acetate, and 20 mM HEPES.KOH, pH 7.4, as described elsewhere[24].

Protein purification. All SNARE and the C2AB domain of synaptotagmin-1 constructs based on rat sequences were expressed in *E. coli* strain BL21 (DE3) and purified by Ni^{2+}-NTA affinity chromatography followed by ion-exchange chromatography as described elsewhere[10,20]. The stabilized Q-SNARE complex consists of syntaxin-1A (aa 183–288) and SNAP-25A (no cysteine, cysteines replaced by alanines) in a 1:1 ratio by the C-terminal VAMP-2 fragment (aa 49–96), and was purified as described earlier[25]. The C2AB domain of synaptotagmin-1 (aa 97–421) and soluble form of VAMP-2 lacking the transmembrane domain ($VAMP\text{-}2_{1-96}$) were purified using a Mono S column (GE Healthcare, Piscataway, NJ) as described previously[26]. The stabilized Q-SNARE complex was purified by Ni^{2+}-NTA affinity chromatography followed by ion-exchange chromatography on a Mono Q column (GE Healthcare, Piscataway, NJ) in the presence of 50 mM n-octyl-β-D-glucoside (OG)[10]. The point mutated C2AB domain (S342C) was labelled with Alexa Fluor 488 C5 maleimide ($C2AB^{A488}$)[26].

Lipid composition of liposomes. All lipids were obtained from Avanti Polar lipids (Alabaster, AL). Lipid composition (mol, %) of the PM-liposomes that contain the Q-SNARE complex was 45% PC (L-α-phosphatidylcholine, Cat. 840055), 15% PE (L-α-phosphatidylethanolamine, Cat. 840026), 10% PS (L-α-phosphatidylserine, Cat. 840032), 25% Chol (cholesterol, Cat. 700000), 4% PI (L-α-phosphatidylinositol, Cat. 840042), and 1% $PI(4,5)P_2$ (PIP_2, Cat. 840046). When PIP_2 concentrations were changed, PI contents were adjusted accordingly. For FRET-based lipid-mixing assays, 1.5% 1,2-dioleoyl-sn-glycero-3-phosphoethanolamine-*N*-(7-nitrobenz-2-oxa-1,3-diazol-4-yl (NBD-DOPE) as a donor dye and 1.5% 1,2-dioleoyl-sn-glycero-3-phosphoethanolamine-*N*-lissamine rhodamine B sulfonyl ammonium salt (Rhodamine-DOPE) as an acceptor dye were incorporated in the PM-liposomes (accordingly 12% unlabelled PE).

Preparation of proteoliposomes. Incorporation of the Q-SNARE complex into large unilamellar vesicles (LUVs) was achieved by OG-mediated reconstitution, called the direct method, i.e. incorporation of proteins into preformed liposomes[10,20]. Briefly, lipids dissolved in a 2:1 chloroform–methanol solvent were mixed according to lipid composition. The solvent was removed using a rotary evaporator to generate lipid film on a glass flask, then lipids were resuspended in 1.5 mL diethyl ether and 0.5 mL buffer containing 150 mM KCl and 20 mM HEPES/KOH pH 7.4. The suspension was sonicated on ice (3 × 45 s), then multilamellar vesicles were prepared by reverse-phase evaporation using a rotary evaporator as diethyl ether was removed. Multilamellar vesicles (0.5 mL) were extruded using polycarbonate membranes of pore size 100 nm (Avanti Polar lipids) to give uniformly-sized LUVs. After the preformed LUVs had been prepared, SNARE proteins were incorporated into them using OG, a mild non-ionic detergent, then the OG was removed by dialysis overnight in 1 L of buffer containing 150 mM KCl and 20 mM HEPES/KOH pH 7.4 together with 2 g SM-2 adsorbent beads. Proteoliposomes had protein-to-lipid molar ratio of 1:500.

Vesicle fusion assay. A FRET-based lipid-mixing assay was applied to monitor vesicle fusion in-vitro[10,20]. LDCV fusion reactions were performed at 37 °C in 1 mL fusion buffer containing 120 mM K-glutamate, 20 mM K-acetate, 20 mM HEPES–KOH (pH 7.4), 1 mM $MgCl_2$, and 3 mM ATP (Fig. 4b). Fusion buffer in Fig. 3a,b contains no ATP, but EGTA; 120 mM K-glutamate, 20 mM K-acetate, 20 mM HEPES–KOH (pH 7.4), 5 mM $MgCl_2$, and 10 µM EGTA. ATP should be made freshly before all experiments, because it is easily destroyed by freezing and thawing. Free Ca^{2+} concentration in the presence of Mg^{2+} and ATP or EGTA was calibrated using the MaxChelator simulation program.

The PM-liposomes that contain NBD-DOPE and Rhodamine-DOPE as a donor and an acceptor dye, respectively, were incubated with LDCVs, thus leading to dequenching of donor fluorescence (NBD) as a result of lipid dilution with unlabelled vesicle membrane[10,20]. The fluorescence dequenching signal of vesicle fusion was measured using wavelength of 460 nm for excitation and 538 nm for emission. Fluorescence values were normalized

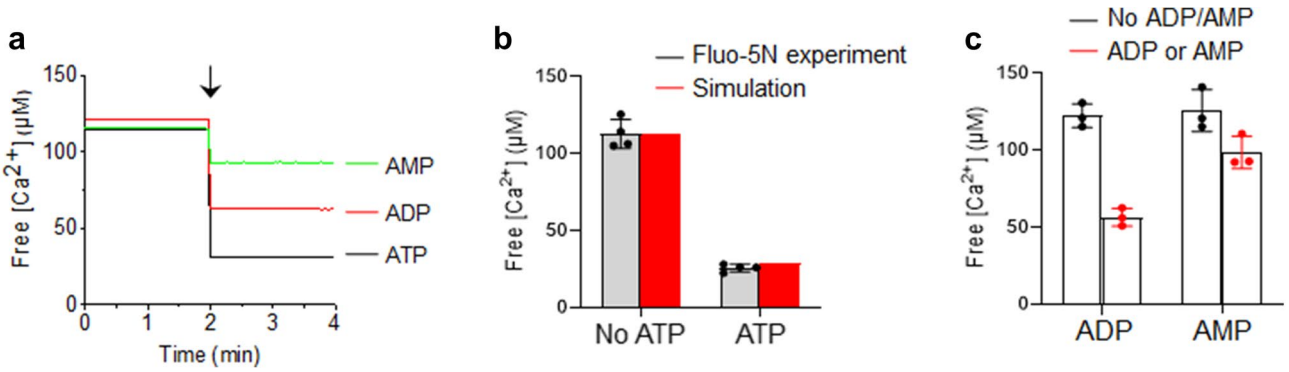

Figure 1. Calibration of free [Ca^{2+}] using Fluo-5N and simulation in the presence of ATP. (**a**) Free [Ca^{2+}] calibration in the presence of ATP, ADP, or AMP using Fluo-5N, a Ca^{2+} indicator with $K_d = 90$ μM. 5 mM of ATP, ADP, or AMP was applied (arrow). Representative trace of free [Ca^{2+}] from four independent experiments. (**b**) Comparison of free [Ca^{2+}] in the presence of 5 mM ATP between Fluo-5N and the MaxChelator simulation program, which calculates free [Ca^{2+}] in the presence of ATP and Mg^{2+}. (**c**) ADP and AMP chelate free [Ca^{2+}], but the Ca^{2+}-chelating efficiency is less than that of ATP. Data in (**b**,**c**) are mean ± SD from three to four independent experiments (n = 3–4).

as a percentage of maximum donor fluorescence (i.e., total fluorescence) after addition of 0.1% Triton X-100 at the end of experiments.

Fluorescence anisotropy measurements. The C2AB fragments (20 nM, S342C) were labelled with Alexa Fluor 488[26]. Anisotropy was measured at 37 °C in 1 mL of buffer containing 120 mM K-glutamate, 20 mM K-acetate, and 20 mM HEPES–KOH (pH 7.4), 5 mM $MgCl_2$, 10 μM EGTA. First, 1 mM Ca^{2+} was applied, then ATP or EGTA was accordingly added to chelate Ca^{2+} and reverse the membrane binding of the C2AB domain; each time ATP or EGTA was uniformly mixed by pipetting and a magnetic stirring setup with dilution factor of 1:500 in 1 mL buffer. (Fig. 2). Excitation wavelength was 495 nm and emission was measured at 520 nm. Anisotropy (r) was calculated using the formula $r = (I_{VV} - G \times I_{VH})/(I_{VV} + 2 \times G \times I_{VH})$, where I_{VV} indicates the fluorescence intensity with vertically polarized excitation and vertical polarization on the detected emission and I_{VH} denotes the fluorescence intensity when using a vertical polarizer on the excitation and horizontal polarizer on the emission. G is a grating factor used as a correction for the instrument's differential transmission of the two orthogonal vector orientations. Lipid composition of the PM-liposomes (protein-free) was identical to those used in a fusion assay except labelled PE (45% PC, 15% PE, 10% PS, 25% Chol, 4% PI, and 1% PIP_2).

Ca^{2+} calibration. ATP contains negatively charged oxygen atoms which bind to Mg^{2+}, Ca^{2+}, or Sr^{2+}, thereby chelating divalent cations[27]. Ca^{2+} concentrations were calibrated with Fluo-5N, pentapotassium salt, cell impermeant, a low-affinity Ca^{2+} indicator with a K_d of 90 μM. Fluo-5N (500 nM) was included in buffer containing 120 mM K-glutamate, 20 mM K-acetate, 20 mM HEPES–KOH (pH 7.4), 5 mM $MgCl_2$, and 10 μM EGTA. 5 mM ATP, ADP, or AMP (sodium salt, Sigma-Aldrich) was added to chelate free Ca^{2+}. The fluorescence signal was measured at 37 °C with wavelength of 494 nm for excitation and 516 nm for emission. The following equation was used to measure free Ca^{2+} concentrations:

$$[Ca^{2+}]_{free} = 90\ \mu M\ (F - F_{min})/(F_{max} - F)$$

where F_{min} is the fluorescence intensity in the absence of calcium with 10 mM EGTA, F_{max} is the maxium fluorescence with 5 mM $CaCl_2$, and F is the fluorescence of intermediate Fluo-5N. Fluo-5N experimental data with 5 mM ATP were correlated with the MaxChelator simulation program that calculates the free [Ca^{2+}].

Statistical analysis. All quantitative data are mean ± SD from ≥ 3 independent experiments. Dose–response curves were fitted using four-parameter logistic equations (4PL) (GraphPad Prism) to calculate Hill slope and EC_{50}.

Results

Calibration of free [Ca^{2+}] using Fluo-5N and simulation program in the presence of ATP. Ca^{2+} is a triggering factor of vesicle fusion and intracellular Ca^{2+} concentration ($[Ca^{2+}]_i$) is typically ~ 100 nM, but local $[Ca^{2+}]_i$ and Ca^{2+} microdomains at the vesicle-release sites close to voltage-gated calcium channels increase to ~ 300 μM[15,28,29]. We used ATP, which is a low affinity Ca^{2+} buffer, to maintain ~ 10 ≤ free [Ca^{2+}] ≤ ~ 300 μM for in-vitro assays[10,20,24,30,31]. ATP has a dissociation constant (K_d) ~ 230 μM [Ca^{2+}][27], so ATP is an excellent Ca^{2+} buffer in the range of 10–500 μM free [Ca^{2+}][32,33]. We used Fluo-5N to measure free [Ca^{2+}] in the presence of ATP to confirm the predictions of [Ca^{2+}] and to determine how much total [Ca^{2+}] is required to achieve a desired free [Ca^{2+}](Fig. 1a–c). Fluo-5N is a low-affinity Ca^{2+} indicator (K_d of 90 μM)[34], which is good for measuring around 100 μM free [Ca^{2+}], because K_d of Ca^{2+} chelators should be close to the desired free [Ca^{2+}][35]. EGTA (10 μM) was

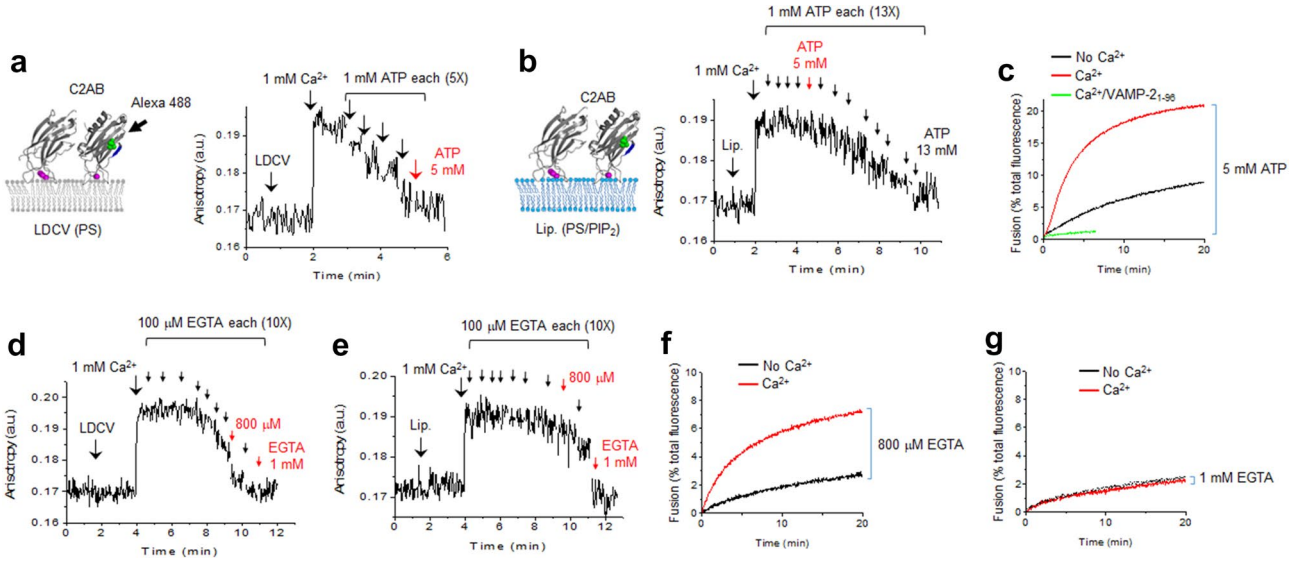

Figure 2. Monitoring *cis*- and *trans*-membrane interaction of synaptotagmin-1. (**a**) Binding of the C2AB domain of synaptotagmin-1 to the membrane of native vesicles (i.e., LDCVs) was monitored using fluorescence anisotropy in which the C2AB domain ($Syt\text{-}1_{97–421}$) was labelled with Alexa Fluor 488 at S342C (green dots). (Left) The C2AB domain has Ca^{2+}-binding sites (magenta) and the Ca^{2+}-bound C2AB domain is inserted to membrane, thus decreasing the rotational mobility. LDCVs contain anionic phospholipids, equivalent to around 15% PS[10]. (Right) A dose of 1 mM Ca^{2+} was applied to induce binding of the C2AB domain to LDCVs, then 1 mM ATP was added five times (arrows) to reverse this binding. The final total of 5 mM ATP disrupted membrane binding of the C2AB domain (red). (**b**) C2AB domain binding to the PM-liposomes. 1 mM ATP was added thirteen times (arrows) and the final total of 13 mM ATP reversed membrane binding of the C2AB domain; the C2AB binding remained in 5 mM ATP (red). (**c**) In-vitro reconstitution of LDCV fusion using a lipid-mixing assay. Purified LDCVs were incubated with the PM-liposomes that incorporate the stabilized Q-SNARE complex. 1 mM Ca^{2+} in the presence of 5 mM ATP accelerated LDCV fusion. (**d**,**e**) Binding of the C2AB domain to LDCVs (**d**) and the PM-liposomes (**e**) was monitored using fluorescence anisotropy as in **a**,**b**. First, 1 mM Ca^{2+} was applied to induce binding of the C2AB domain, then 100 μM EGTA was added ten times (arrows) to reverse this binding. A total dose of 800 μM EGTA disrupted C2AB binding to LDCV (red, **d**) and a final total dose of 1 mM EGTA reversed C2AB binding to liposomes (red, **e**). (**f**,**g**) LDCV fusion was increased by 1 mM Ca^{2+} in the presence of 800 μM EGTA (**f**), but was not affected in the presence of 1 mM EGTA (**g**).

included to remove contaminating Ca^{2+} for the calibration of free [Ca^{2+}]. An initial total 113 μM free [Ca^{2+}] was reduced to 26 μM in the presence of 5 mM ATP by its chelation of Ca^{2+} (Fig. 1a,b).

Then we compared this experimental data of free [Ca^{2+}] with the MaxChelator, which is a computer simulation programs[32,35] that enables calculation of appropriate stoichiometric concentrations of Ca^{2+} and Mg^{2+} in the presence of different Ca^{2+} chelators such as EGTA and ATP, and thereby provides detailed infomation to obtain the desired free [Ca^{2+}][35]. The MaxChelator program included 5 mM Mg^{2+} and 10 μM EGTA, and assumed 37 °C as in the Ca^{2+} calibration experiments (Fig. 1a). Indeed the MaxChelator calculated free [Ca^{2+}] = 29 μM in the presence of 5 mM ATP with 113 μM total [Ca^{2+}] at pH 7.4. This agreement with the measured free [Ca^{2+}] = 26 μM confirms that the MaxChelator can predict free [Ca^{2+}] obtained in experiments that use a Fluo-5N fluorescent Ca^{2+} indicator (Fig. 1b).

Negatively-charged oxygen atoms of ATP chelate divalent cations such as Mg^{2+}, Ca^{2+}, or Sr^{2+}[27]. In the experiments, 5 mM ADP or 5 mM AMP chelated Ca^{2+}, thereby reducing free [Ca^{2+}] from 122 to 57 μM and from 126 to 99 μM, respectively (Fig. 1c). Increasing the number of phosphate groups in Adenosine increases Ca^{2+} affinity and lowers K_d by increasing the number of Ca^{2+} ions that are bound[27,33]. ATP, ADP, and AMP have distinct ranges of Ca^{2+}-buffering capacity and distinct K_d values[33], so Ca^{2+}-chelating effect is ATP > ADP > AMP (Fig. 1a–c). Altogether, the predictions of free [Ca^{2+}] in the complex buffer solutions including Mg^{2+}, ATP and EGTA were confirmed using a fluorescent Ca^{2+} indicator.

Monitoring the *cis*- and *trans*-membrane interaction of synaptotagmin-1. Synaptotagmin-1 interacts with anionic phospholipids by electrostatic interaction. Native vesicles contain ~ 15% anionic phospholipids, including phosphatidylserine (PS) and phosphatidylinositol (PI)[6]. Therefore, Ca^{2+} induces synaptotagmin-1 to bind to its own vesicle membrane, i.e., *cis*-interaction, which prevents *trans*-interaction to the plasma membranes and thereby inactivates the ability of synaptotagmin-1 to trigger fusion[7–9].

Ca^{2+}-bound synaptotagmin-1 is inserted to native vesicle membranes such as synaptic vesicles and large dense-core vesicles (LDCVs) that contain anionic phospholipids[10]. However, ATP electrostatically prevents the *cis*-interaction of synaptotagmin-1, whereas the *trans*-interaction of synaptotagmin-1 to the plasma membrane remains active to mediate Ca^{2+}-dependent vesicle fusion, because PIP_2 overcomes the inhibitory effect of ATP by increasing the membrane-binding affinity of the C2AB domain[10–12].

ATP concentration [mM]	Free Ca^{2+} [μM] (total 1 mM Ca^{2+})[b]	EGTA concentration [μM]	Free Ca^{2+} [μM] (total 1 mM Ca^{2+})
1	896	100	900
2	785	200	800
4	508	300	700
5	351	800	200
13	31	1000	12

Table 1. Calibration of free Ca^{2+} concentration in the presence of ATP or EGTA[a]. [a]The MaxChelator simulation program was used to calculate free Ca^{2+} concentration in the presence of ATP or EGTA. [b]1 mM Ca^{2+}, 5 mM Mg^{2+}, and 10 μM EGTA.

We tested an assay that uses fluorescence anisotropy measurement to monitor the *cis*- and *trans*-membrane interaction of synaptotagmin-1 (Fig. 2). Direct measurement of the *cis*- and *trans*-membrane interaction of endogenous synaptotagmin-1 in native vesicle membranes is impossible, so we monitored the binding of an exogenously-added C2AB domain of synaptotagmin-1 (Syt_{97-421}), which was labelled with Alexa Fluor 488 at S342C (Fig. 2a). We took advantage of a single fluorescent labelling for anisotropy measurement to monitor the interaction of the C2AB domain with native vesicles or liposomes; the membrane-bound C2AB domain leads to increase of fluorescence anisotropy due to a reduction in the rotational mobility[10] (Fig. 2a,b). It is noted that our experiments using the cytoplasmic C2AB domain are intended to shed light on the *cis*- and *trans*-interactions, but the geometry is not truly being imitated.

We first monitored the *cis*-membrane interaction between the C2AB domain and the LDCV membranes (Fig. 2a). The presence of 1 mM Ca^{2+} increased fluorescence anisotropy; this change indicates that the C2AB domains bind to LDCV membranes in a Ca^{2+}-dependent manner. Five sequential applications of 1 mM ATP gradually decreased the anisotropy signal by chelating Ca^{2+}; this result suggests dissociation of the C2AB domain from LDCVs (Fig. 2a). 5 mM ATP in the presence of 1 mM Ca^{2+} almost completely disrupted the *cis*-membrane interaction of the C2AB domain with the LDCV membranes (Fig. 2a); free [Ca^{2+}] in the presence of Mg^{2+}, ATP and EGTA was calibrated using the MaxChelator simulation program and free [Ca^{2+}] was 351 μM in case of 5 mM ATP and 1 mM Ca^{2+} (Table 1).

Next, we tested the *trans*-membrane interactions between the C2AB domain and the PM-liposomes; 10% PS, 4% PI, and 1% PIP_2 were included in the PM-liposomes (Fig. 2b). The C2AB domain of synaptotagmin-1 bound to liposomes in response to 1 mM Ca^{2+}, and this *trans*-membrane interaction was reduced by ATP, 1 mM applied thirteen times sequentially (Fig. 2b). Free [Ca^{2+}] in different ATP concentrations was summarized in Table 1. Ca^{2+}-dependent vesicle fusion is accelerated by the increase of the *trans*-interactions and the decrease of the *cis*-membrane interaction of synaptotagmin-1[10,20], so we hypothesized that 5 mM ATP in the presence of 1 mM Ca^{2+} is appropriate to observe Ca^{2+}-dependent fusion (red in Fig. 1a,b).

To test this hypothesis and examine the effect of the *cis*- and *trans*-membrane interaction of synaptotagmin-1 on vesicle fusion, we applied a reconstitution system of vesicle fusion by using native LDCVs[10,20,24]. The PM-liposomes contain the stabilized Q-SNARE complex (syntaxin-1A and SNAP-25A in a 1:1 molar ratio[25]). Indeed, 5 mM ATP in the presence of 1 mM Ca^{2+} (i.e., 351 μM free [Ca^{2+}] according to the MaxChelator program (Table 1)) dramatically accelerated LDCV fusion, which was completely blocked by the soluble VAMP-2 ($VAMP\text{-}2_{1-96}$); this results indicates SNARE-dependent vesicle fusion (Fig. 2c). We have previously shown that 300–400 μM free [Ca^{2+}] in the absence of ATP fails to enhance vesicle fusion, but rather slightly inhibits fusion, because the *cis*-membrane interaction of the C2AB domain to native vesicle membranes becomes robust from 100 μM up to 3 mM[10]. ATP prevents this *cis*-membrane interaction by charge screening and competing with the vesicle membrane, thus allowing synaptotagmin-1 to interact in *trans* with the plasma membrane[10].

Polyphosphates such as ATP reverse an inactivating *cis*-interaction of synaptotagmin-1 by an electrostatic effect (Fig. 2a–c). Next, we tested whether other Ca^{2+} chelators, e.g., EGTA, can have a similar inhibitory effect on the *cis*-membrane interaction. Anisotropy measurement was performed to monitor the *cis*- and *trans*-membrane interaction of the C2AB domain (Fig. 2a,b). EGTA was applied 10 times (100 μM each in the presence of 1 mM Ca^{2+}) to reverse the *cis*-interaction of the C2AB domain to LDCVs (Fig. 2d). Application of 800 μM EGTA dramatically disrupted the *cis*-interaction in the presence of total 1 mM Ca^{2+} (red in Fig. 2d); free [Ca^{2+}] was 200 μM (Table 1). However, the *trans*-membrane interactions of the C2AB domain to the PM-liposomes remained robust in the presence of 800 μM EGTA with 1 mM Ca^{2+} (200 μM free [Ca^{2+}], Fig. 2e), whereas 1 mM EGTA significantly disrupted both the *cis*- and *trans*-membrane interactions of the C2AB domain (Fig. 2d,e); free [Ca^{2+}] was 12 μM (Table 1).

Anisotropy measurement is useful to find a Ca^{2+}-buffering condition to observe Ca^{2+}-dependent vesicle fusion, where the *cis*-membrane interaction is prevented and the *trans*-interaction remains active. The presence of 800 μM EGTA with 1 mM Ca^{2+} (200 μM free [Ca^{2+}], Table 1) significantly reversed the *cis*-interaction (Fig. 2d), but had a minor effect on the *trans*-interaction (Fig. 2e). Indeed, 800 μM EGTA with 1 mM Ca^{2+} reproduced Ca^{2+}-dependent LDCV fusion (Fig. 2f). 1 mM EGTA with 1 mM Ca^{2+} (12 μM free [Ca^{2+}], Table 1) failed to accelerate fusion, because the *trans*-interaction of the C2AB domain was dramatically disrupted by 1 mM EGTA (red in Fig. 2e); it is mainly because of low free [Ca^{2+}]. Taken together, we established an anisotropy assay to monitor the *cis*- and *trans*-membrane interaction of synaptotagmin-1 by using native LDCVs and the PM-liposomes. Our data suggest that Ca^{2+} chelators such as EGTA, in addition to polyphosphates such as ATP, can prevent the *cis*-membrane interaction of synaptotagmin-1 by the electrostatic effect in a certain range of free [Ca^{2+}].

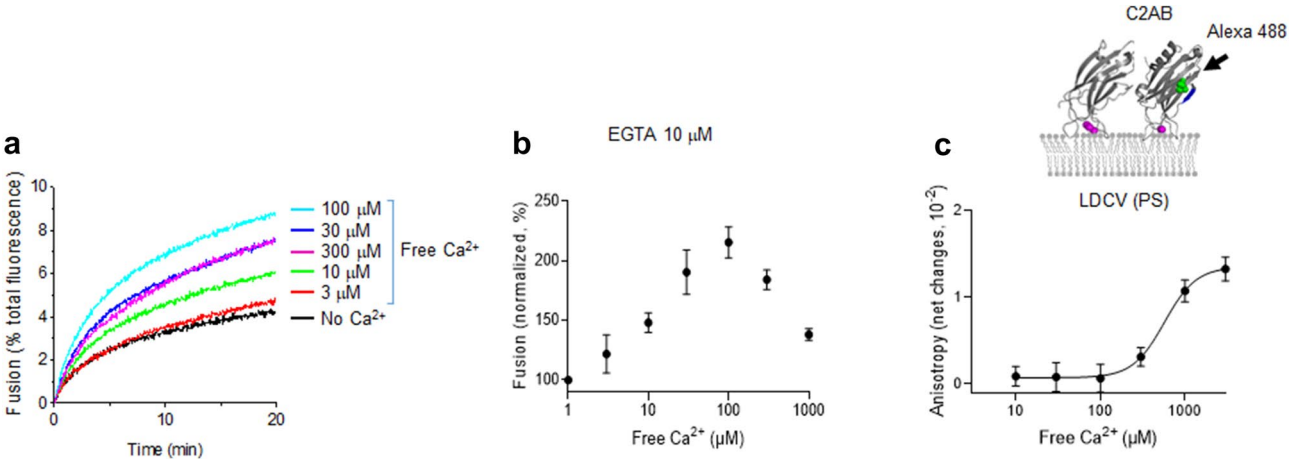

Figure 3. EGTA reproduces ATP effect on Ca^{2+}-dependent LDCV fusion and the C2AB binding to LDCVs. (**a**,**b**) LDCV fusion using a lipid-mixing assay as described in Fig. 2c at different concentrations of Ca^{2+} in the presence of 10 μM EGTA, instead of ATP. (**a**) Representative trace of dequenching of donor fluorescence (NBD). (**b**) Dose–response curve of LDCV fusion at various free [Ca^{2+}]. Fusion is normalized as a percentage of control (No Ca^{2+}). (**c**) Ca^{2+} dose–response curve for C2AB binding to LDCVs in the presence of 10 μM EGTA using anisotropy as described in Fig. 2a. Data in (**b**,**c**) are mean ± SD from three independent experiments (n = 3). Free [Ca^{2+}] were calibrated using the MaxChelator simulation program. (**a**–**c**) ATP was not included in buffer: 120 mM K-glutamate, 20 mM K-acetate, 20 mM HEPES–KOH (pH 7.4), 5 mM $MgCl_2$, and 10 μM EGTA.

EGTA reproduces the biphasic regulation of Ca^{2+} on LDCV fusion. We have previously reported the biphasic regulation of Ca^{2+} on LDCV fusion; 10–100 μM free Ca^{2+} exponentially accelerates native vesicle fusion, but > 300 μM free [Ca^{2+}] progressively reduces Ca^{2+}-dependent fusion, showing biphasic regulation of Ca^{2+} on LDCV fusion in a bell-shaped dose-dependence[20]. ATP was used for Ca^{2+}-buffering to maintain free [Ca^{2+}] in the range of 10–500 μM[20]. We examined whether EGTA reproduces the biphasic regulation of Ca^{2+} on LDCV fusion (Fig. 3a,b). Instead of ATP, 10 μM EGTA was included in fusion buffer and free [Ca^{2+}] was calculated using the MaxChelator program. As expected, biphasic regulation of Ca^{2+} on LDCV fusion was observed, where Ca^{2+}-dependent fusion progressively increased until [Ca^{2+}] = ~ 100 μM, and gradually decreased at [Ca^{2+}] from 300 μM to 1 mM (Fig. 3a,b).

Biphasic regulation of Ca^{2+} on LDCV fusion is mediated by two different mechanisms: (1) millimolar range of [Ca^{2+}] decreases the *trans*-interaction of synaptotagmin-1 by shielding PIP_2 and (2) sub-millimolar range of [Ca^{2+}] above 300 μM increases the *cis*-interaction of synaptotagmin-1 to its own vesicle membrane[20]. To further confirm the *cis*-interaction at higher [Ca^{2+}], we performed anisotropy measurement (Fig. 2a,d) to study the Ca^{2+} dose–response of the *cis*-interaction of synaptotagmin-1 in the presence of EGTA instead of ATP (Fig. 3c). Indeed, the *cis*-membrane interaction of the C2AB domain gradually increased from 300 μM [Ca^{2+}] and remained robust at millimolar [Ca^{2+}](Fig. 3c). Note that ATP and EGTA give rise to different kinetics of the Ca^{2+} dose–response curves of vesicle fusion and the *cis*-interaction of synaptotagmin-1[20], because ATP effectively buffers free [Ca^{2+}] in the range of 10–500 μM, but EGTA cannot efficiently buffer free [Ca^{2+}] in this range.

PIP_2 concentration regulates Ca^{2+} cooperativity of synaptotagmin-1. Synaptotagmin-1 binds to anionic phospholipids by electrostatic interaction and the Ca^{2+}-binding loops of the C2 domains are inserted to anionic phospholipids in a Ca^{2+}-dependent manner; aspartate residues of the Ca^{2+}-binding loops in the C2-domains together with anionic membrane lipids coordinate Ca^{2+}-ions[21,23,36]. PIP_2 enhances Ca^{2+}-sensitivity of synaptotagmin-1 by interacting with the polybasic patch in the C2B domain[10,21]. Ca^{2+}-cooperativity of synaptotagmin-1 varies among cell types, with the Hill coefficients ranging from ~ 2 to ~ 5. We tested that PIP_2 also regulates Ca^{2+}-cooperativity of synaptotagmin-1 for membrane binding (Fig. 4a, Table 2) and vesicle fusion (Fig. 4b, Table 2). Increases of PIP_2 concentration from 1 to 5% in the PM-liposomes shifted Ca^{2+} titration curves for membrane binding to the left side; this change indicates increased Ca^{2+} sensitivity, but reduced Ca^{2+} cooperativity (Fig. 4a, Table 2).

Next, we observed that Ca^{2+}-cooperativity of synaptotagmin-1 for vesicle fusion was also reduced by increasing PIP_2 concentration, correlating with the Ca^{2+}-cooperativity of synaptotagmin-1 for membrane binding. The Ca^{2+} dose–response curve for LDCV fusion was shifted leftward as PIP_2 concentration was increased in the PM-liposomes (Fig. 4b, Table 2). Taken together, high PIP_2 concentration increases the sensitivity of synaptotagmin-1 to Ca^{2+}, but lowers Ca^{2+} cooperativity. These changes imply that increasing the negative electrostatic potential in the plasma membranes attracts Ca^{2+}-bound synaptotagmin-1 with low Ca^{2+} cooperativity, in which the total numbers of Ca^{2+} ions coordinated to one synaptotagmin-1 might be reduced to 2–3 (see section "Discussion").

Discussion

The *cis*-binding of synaptotagmin-1 occurs in native vesicles such as LDCVs and synaptic vesicles, and inactivates Ca^{2+}-dependent vesicle fusion by preventing the *trans*-interaction of synaptotagmin-1. Independent groups have confirmed that ATP at physiological concentrations disrupts such *cis*-interaction of synaptotagmin-1[11,12,37].

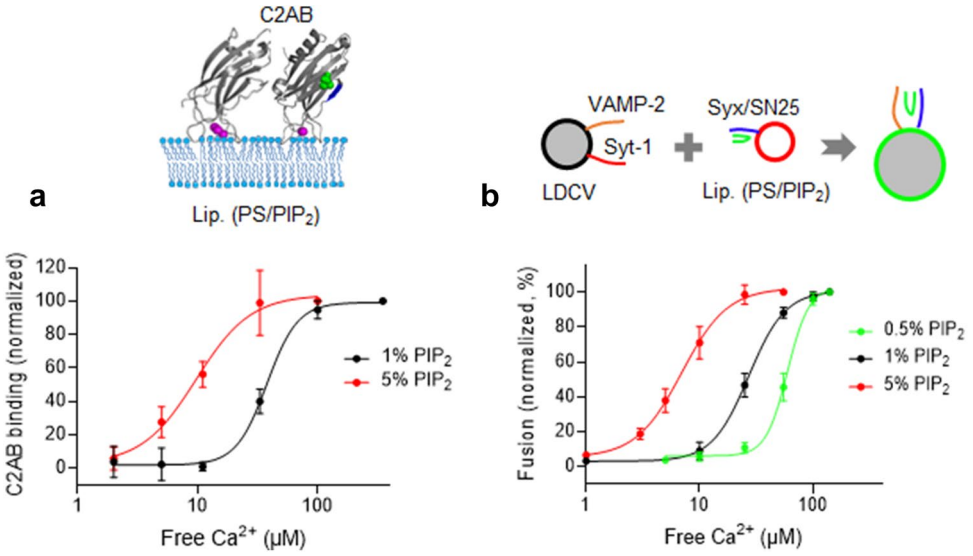

Figure 4. PIP_2 concentration regulates Ca^{2+} sensitivity and cooperativity of synaptotagmin-1. (**a**) Membrane binding of the C2AB domain of synaptotagmin-1 was monitored using anisotropy as in Fig. 2b. Ca^{2+} dose–response curve for C2AB binding to the PM-liposomes that include PS and PIP_2. C2AB binding is presented as a percentage of maximum C2AB binding. (**b**) Ca^{2+} dose–response curve for LDCV fusion with the PM-liposomes containing different PIP_2 concentrations. Fusion is normalized as a percentage of maximum fusion. Data in (**a**,**b**) are mean ± SD from three independent experiments (n = 3). 3 mM $MgCl_2$ and 1 mM ATP were included in buffer, and free $[Ca^{2+}]$ was calibrated using the MaxChelator simulation program.

Methods	Synaptotagmin-1	Hill slope†	EC_{50} (μM) †	Anionic phospholipids (%)‡
Anisotropy	C2AB	3.39 ± 1.29	37.7 ± 2.9	PIP_2 (1), PS (15), PI (4)
	C2AB	1.92 ± 0.7	9.7 ± 1.7	PIP_2 (5), PS (15)
Fusion (LDCV and liposomes)	Full length[a]	4.57 ± 1.14	59.4 ± 2.47	PIP_2 (0.5), PS (15), PI (4.5)
	Full length	2.69 ± 0.08	27.1 ± 0.29	PIP_2 (1), PS (15), PI (4)
	Full length	2.16 ± 0.18	6.96 ± 0.29	PIP_2 (5), PS (15)

Table 2. Hill slope and EC_{50} of Ca^{2+} dose–response curve. †Hill slope and EC_{50} of Ca^{2+} dose–response curve were calculated using four-parameter logistic equations in GraphPad Prism. Data in the table are means ± SE (standard error) from three to five independent experiments. All experiments were carried out in buffer containing 3 mM ATP and 1 mM $MgCl_2$ (section "Material and methods"). ‡Lipid compositions of anionic phospholipids in liposomes. [a]Endogenous synaptotagmin-1 from purified native LDCVs.

Here we show that Ca^{2+} chelators, including EGTA and polyphosphate anions such as ATP, ADP, and AMP, electrostatically reverse the *cis*-interaction of synaptotagmin-1. We propose that Ca^{2+} chelators compete with vesicle membranes that contain anionic phospholipids in binding to Ca^{2+} and disrupt the *cis*-interaction of synaptotagmin-1 by charge screening[10]. However, PIP_2 overcomes this inhibitory effect of ATP, because PIP_2 dramatically enhances the Ca^{2+}-binding affinity of synaptotagmin-1[21,38]; this high Ca^{2+} affinity of the C2AB domain to PIP_2-containing membranes is not affected by ATP[10].

EGTA and 1,2-bis(o-aminophenoxy)ethane-N,N,N0,N0-tetraacetic acid (BAPTA) are well-known and reliable Ca^{2+} buffers in the range of 10 nM–1 μM $[Ca^{2+}]$ at the typical intracellular pH of 7.2[33,35]. Given that EGTA and BAPTA have a K_d of 67 nM and 192 nM $[Ca^{2+}]$ at pH 7, respectively, and have a higher affinity for Ca^{2+} than for Mg^{2+}[35], both EGTA and BAPTA effectively buffer free $[Ca^{2+}]$ only at concentrations < 1 μM[33,39], which is close to intracellular free $[Ca^{2+}]$. However, EGTA is sensitively dependent on pH[35], and BAPTA family has a strong dependence on ionic strength[40]; importantly, because EGTA and BAPTA have nanomolar-level K_d, they poorly buffer free $[Ca^{2+}]$ in the range of 10–500 μM. In contrast, ATP has K_d 230 μM[27] and is an excellent buffer for free $[Ca^{2+}]$ in the range of 10–500 μM[33].

Synaptotagmin-1 is a low-affinity Ca^{2+} sonsor; 10–100 μM $[Ca^{2+}]$ exponentially induce synaptotagmin-1 binding to membrane that contain PS and PIP_2 with $K_d \sim 50$ μM[21,26]. Therefore, ATP is an appropriate and better Ca^{2+} buffer than EGTA or BAPTA to study the synaptotagmin-1 activity to bind membrane and trigger vesicle fusion. Indeed, we oberserved that ATP and EGTA result in different kinetics of the Ca^{2+} dose–response curves of vesicle fusion and of the *cis*-interaction of synaptotagmin-1[10,20] (Fig. 3b,c), because ATP has a different Ca^{2+}-buffering capacity than EGTA.

The K_d of low-affinity Ca^{2+} indicator dyes can vary depending on ionic strength and is changed by anions such as ATP[41]; e.g., the K_d of low-affinity Ca^{2+} indicator dyes is increased by ATP and slightly decreased by excess Mg^{2+}. The K_d of Fluo-5N can be altered by the presence of ATP/Mg^{2+}, which makes it difficult to accurately measure free [Ca^{2+}]. ATP binds both Ca^{2+} and Mg^{2+} with a different affinity[27,33], so computer simulation programs[32,35] like the MaxChelator are useful to calibrate free [Ca^{2+}] in the presence of Mg^{2+}, ATP or EGTA by calculating free [Mg^{2+}], [Ca-ATP], and [Mg-ATP][35]. We confirmed the MaxChelator-based predictions using a Fluo-5N fluorescent Ca^{2+} indicator (Fig. 1b).

Both the C2A and C2B domains of synaptotagmin-1 have highly cooperative Ca^{2+}-dependent binding to membranes that contain anionic phospholipids[26,42–45]. Furthermore, synaptotagmin-1 contains a polybasic region within the C2B domain that binds to PIP_2 in an Ca^{2+}-independent manner[46,47] and enhances Ca^{2+} sensitivity of synaptotagmin-1 membrane binding[21] and exocytosis[48]. The C2AB domain has five possible Ca^{2+}-binding sites[22,23]; negatively charged oxygen atom from acidic aspartate residues in the C2AB domain and negatively charged oxygen atom from anionic phospholipids provide complete coordination sites for Ca^{2+}[23,36]. Ca^{2+} cooperativity of the C2AB domain seems reasonable when the Hill coefficient is ~ 4 to 5, but what regulates Ca^{2+} cooperativity remains poorly understood, e.g., low Hill coefficient (n, 2–3) in neuroendocrine cells such as pituitary melanotrophs (n, 2.5)[18] and chromaffin cells (n, 1.8)[19], but high Hill coefficient in synapses including calyx-of-Held synapses (n, 4.2)[13–15], neuromuscular junctions (n, 3.8)[16], and bipolar cells (n, 4)[17]. We overserved that increasing PIP_2 concentration reduces the Hill coefficient, which represents Ca^{2+} cooperativity (Fig. 4). Our data support that local PIP_2 concentration might control Ca^{2+} cooperativity by allosterically-stabilized dual binding of synaptotagmin-1 to Ca^{2+} and PIP_2[38].

In this study, we investigate the electrostatic regulation of C2AB binding to vesicle membrane and the PM-liposomes. We have previously observed that Ca^{2+}-independent interactions of the C2AB domain with the PM-liposomes containing anionic phospholipids (10% PS/1% PIP_2) is significantly disrupted in the presence of physiological concentration of ATP/Mg^{2+}, but this Ca^{2+}-independent interaction remains strong when the PM-liposomes contain high PIP_2 (10% PS/5% PIP_2), suggesting that high PIP_2 concentrations are required for Ca^{2+}-independent binding of the C2AB domain in physiological ionic strength[20]. Here, we have used 10% PS/1% PIP_2 in the PM-liposomes to selectively examine the Ca^{2+}-dependent membrane interaction and binding of the C2AB domain. However, in the pre-fusion state for vesicle docking and priming, the C2AB domain of synaptotagmin-1 is most likely bound to the plasma membrane through the PIP_2-interacting polybasic region of the C2B domain[20] or the SNARE complex[49] in a Ca^{2+}-independent manner. Ca^{2+} can induce a re-orientation of the C2AB domain on the plasma membrane by changing the binding mode with the SNARE complex[49] or PIP_2[45]. This change in orientation may act as a switch to trigger synaptotagmin-1-dependent vesicle fusion in neurons and neuroendocrine cells. Our results do not rule out the possibility for Ca^{2+}-independent interactions of synaptotagmin-1 with the SNARE complex despite extremely weak interaction[49] and it remains a topic of further study to include Ca^{2+}-independent interactions of synaptotagmin-1 in our system for physiological relevance.

Data availability

The datasets generated during the current study are available from the corresponding author on reasonable requests.

Received: 15 September 2022; Accepted: 19 December 2022
Published online: 27 December 2022

References

1. Jahn, R. & Scheller, R. H. SNAREs—engines for membrane fusion. *Nat. Rev. Mol. Cell Biol.* **7**, 631–643 (2006).
2. Brunger, A. T., Choi, U. B., Lai, Y., Leitz, J. & Zhou, Q. Molecular mechanisms of fast neurotransmitter release. *Annu. Rev. Biophys.* **47**, 469–497 (2018).
3. Ramakrishnan, N. A., Drescher, M. J. & Drescher, D. G. The SNARE complex in neuronal and sensory cells. *Mol. Cell Neurosci.* **50**, 58–69 (2012).
4. Shao, X. *et al.* Synaptotagmin-syntaxin interaction: The C2 domain as a Ca2+-dependent electrostatic switch. *Neuron* **18**, 133–142 (1997).
5. Park, Y. & Ryu, J. K. Models of synaptotagmin-1 to trigger Ca(2+) -dependent vesicle fusion. *FEBS Lett.* **592**, 3480–3492 (2018).
6. Takamori, S. *et al.* Molecular anatomy of a trafficking organelle. *Cell* **127**, 831–846 (2006).
7. Stein, A., Radhakrishnan, A., Riedel, D., Fasshauer, D. & Jahn, R. Synaptotagmin activates membrane fusion through a Ca2+-dependent trans interaction with phospholipids. *Nat. Struct. Mol. Biol.* **14**, 904–911 (2007).
8. Vennekate, W. *et al.* Cis- and trans-membrane interactions of synaptotagmin-1. *Proc. Natl. Acad. Sci. U S A* **109**, 11037–11042 (2012).
9. Holt, M., Riedel, D., Stein, A., Schuette, C. & Jahn, R. Synaptic vesicles are constitutively active fusion machines that function independently of Ca2+. *Curr. Biol.* **18**, 715–722 (2008).
10. Park, Y. *et al.* Controlling synaptotagmin activity by electrostatic screening. *Nat. Struct. Mol. Biol.* **19**, 991–997 (2012).
11. Nyenhuis, S. B., Thapa, A. & Cafiso, D. S. Phosphatidylinositol 4,5 Bisphosphate Controls the cis and trans Interactions of Synaptotagmin 1. *Biophys. J.* **117**, 247–257 (2019).
12. Dietz, J. *et al.* Forces, kinetics, and fusion efficiency altered by the full-length synaptotagmin-1-PI(4,5)P2 interaction in constrained geometries. *Nano Lett.* **22**, 1449–1455 (2022).
13. Sun, J. *et al.* A dual-Ca^{2+}-sensor model for neurotransmitter release in a central synapse. *Nature* **450**, 676–682 (2007).
14. Lou, X., Scheuss, V. & Schneggenburger, R. Allosteric modulation of the presynaptic Ca^{2+} sensor for vesicle fusion. *Nature* **435**, 497–501 (2005).
15. Schneggenburger, R. & Neher, E. Intracellular calcium dependence of transmitter release rates at a fast central synapse. *Nature* **406**, 889–893 (2000).
16. Dodge, F. A. Jr. & Rahamimoff, R. Co-operative action a calcium ions in transmitter release at the neuromuscular junction. *J. Physiol.* **193**, 419–432 (1967).
17. Heidelberger, R., Heinemann, C., Neher, E. & Matthews, G. Calcium dependence of the rate of exocytosis in a synaptic terminal. *Nature* **371**, 513–515 (1994).

18. Thomas, P., Wong, J. G., Lee, A. K. & Almers, W. A low affinity Ca2+ receptor controls the final steps in peptide secretion from pituitary melanotrophs. *Neuron* **11**, 93–104 (1993).
19. Augustine, G. J. & Neher, E. Calcium requirements for secretion in bovine chromaffin cells. *J. Physiol.* **450**, 247–271 (1992).
20. Park, Y. *et al.* Synaptotagmin-1 binds to PIP(2)-containing membrane but not to SNAREs at physiological ionic strength. *Nat. Struct. Mol. Biol.* **22**, 815–823 (2015).
21. Perez-Lara, A. *et al.* PtdInsP2 and PtdSer cooperate to trap synaptotagmin-1 to the plasma membrane in the presence of calcium. *Elife* **5**, 25 (2016).
22. Fernandez, I. *et al.* Three-dimensional structure of the synaptotagmin 1 C2B-domain: Synaptotagmin 1 as a phospholipid binding machine. *Neuron* **32**, 1057–1069 (2001).
23. Ubach, J., Zhang, X., Shao, X., Sudhof, T. C. & Rizo, J. Ca2+ binding to synaptotagmin: How many Ca2+ ions bind to the tip of a C2-domain?. *EMBO J.* **17**, 3921–3930 (1998).
24. Birinci, Y., Preobraschenski, J., Ganzella, M., Jahn, R. & Park, Y. Isolation of large dense-core vesicles from bovine adrenal medulla for functional studies. *Sci. Rep.* **10**, 7540 (2020).
25. Pobbati, A. V., Stein, A. & Fasshauer, D. N- to C-terminal SNARE complex assembly promotes rapid membrane fusion. *Science* **313**, 673–676 (2006).
26. Radhakrishnan, A., Stein, A., Jahn, R. & Fasshauer, D. The Ca2+ affinity of synaptotagmin 1 is markedly increased by a specific interaction of its C2B domain with phosphatidylinositol 4,5-bisphosphate. *J. Biol. Chem.* **284**, 25749–25760 (2009).
27. Wilson, J. E. & Chin, A. Chelation of divalent cations by ATP, studied by titration calorimetry. *Anal. Biochem.* **193**, 16–19 (1991).
28. Llinas, R., Sugimori, M. & Silver, R. B. Microdomains of high calcium concentration in a presynaptic terminal. *Science* **256**, 677–679 (1992).
29. Parekh, A. B. Ca2+ microdomains near plasma membrane Ca2+ channels: Impact on cell function. *J. Physiol.* **586**, 3043–3054 (2008).
30. Park, Y. *et al.* alpha-SNAP interferes with the zippering of the SNARE protein membrane fusion machinery. *J. Biol. Chem.* **289**, 16326–16335 (2014).
31. Gumurdu, A. *et al.* MicroRNA exocytosis by large dense-core vesicle fusion. *Sci. Rep.* **7**, 45661 (2017).
32. Schoenmakers, T. J., Visser, G. J., Flik, G. & Theuvenet, A. P. CHELATOR: An improved method for computing metal ion concentrations in physiological solutions. *Biotechniques* **12**(870–874), 876–879 (1992).
33. Patton, C., Thompson, S. & Epel, D. Some precautions in using chelators to buffer metals in biological solutions. *Cell Calcium* **35**, 427–431 (2004).
34. Kabbara, A. A. & Allen, D. G. The use of the indicator fluo-5N to measure sarcoplasmic reticulum calcium in single muscle fibres of the cane toad. *J. Physiol.* **534**, 87–97 (2001).
35. Bers, D. M., Patton, C. W. & Nuccitelli, R. A practical guide to the preparation of Ca(2+) buffers. *Methods Cell Biol.* **99**, 1–26 (2010).
36. Murray, D. & Honig, B. Electrostatic control of the membrane targeting of C2 domains. *Mol. Cell* **9**, 145–154 (2002).
37. Zanetti, M. N. *et al.* Ring-like oligomers of Synaptotagmins and related C2 domain proteins. *Elife* **5**, 25 (2016).
38. Kobbersmed, J. R. L., Berns, M. M. M., Ditlevsen, S., Sorensen, J. B. & Walter, A. M. Allosteric stabilization of calcium and phosphoinositide dual binding engages several synaptotagmins in fast exocytosis. *Elife* **11**, 20 (2022).
39. Bers, D. M. A simple method for the accurate determination of free [Ca] in Ca-EGTA solutions. *Am. J. Physiol.* **242**, C404-408 (1982).
40. Tsien, R. Y. New calcium indicators and buffers with high selectivity against magnesium and protons: Design, synthesis, and properties of prototype structures. *Biochemistry* **19**, 2396–2404 (1980).
41. Woehler, A., Lin, K. H. & Neher, E. Calcium-buffering effects of gluconate and nucleotides, as determined by a novel fluorimetric titration method. *J. Physiol.* **592**, 4863–4875 (2014).
42. Chapman, E. R. How does synaptotagmin trigger neurotransmitter release?. *Annu. Rev. Biochem.* **77**, 615–641 (2008).
43. Davletov, B. A. & Sudhof, T. C. A single C2 domain from synaptotagmin I is sufficient for high affinity Ca2+/phospholipid binding. *J. Biol. Chem.* **268**, 26386–26390 (1993).
44. Tran, H. T., Anderson, L. H. & Knight, J. D. Membrane-binding cooperativity and coinsertion by C2AB tandem domains of synaptotagmins 1 and 7. *Biophys. J.* **116**, 1025–1036 (2019).
45. Katti, S., Nyenhuis, S. B., Her, B., Cafiso, D. S. & Igumenova, T. I. Partial metal ion saturation of C2 domains primes synaptotagmin 1-membrane interactions. *Biophys. J.* **118**, 1409–1423 (2020).
46. Kuo, W., Herrick, D. Z., Ellena, J. F. & Cafiso, D. S. The calcium-dependent and calcium-independent membrane binding of synaptotagmin 1: Two modes of C2B binding. *J. Mol. Biol.* **387**, 284–294 (2009).
47. Vrljic, M. *et al.* Post-translational modifications and lipid binding profile of insect cell-expressed full-length mammalian synaptotagmin 1. *Biochemistry* **50**, 9998–10012 (2011).
48. Li, L. *et al.* Phosphatidylinositol phosphates as co-activators of Ca2+ binding to C2 domains of synaptotagmin 1. *J. Biol. Chem.* **281**, 15845–15852 (2006).
49. Rizo, J., David, G., Fealey, M. E. & Jaczynska, K. On the difficulties of characterizing weak protein interactions that are critical for neurotransmitter release. *FEBS Open Bio* **12**, 1912–1938 (2022).

Acknowledgements

This work was supported by the grant from Qatar Biomedical Research Institute (Project Number SF 2019 004 to Y.P.).

Author contributions

Y.P. and H.Y.A.M. purified vesicles and performed experiments. Y.P. collected and analyzed data. Y.P. wrote the manuscript and all authors read and provided their comments.

Funding

Open Access funding was provided by the Qatar National Library.

Competing interests

The authors declare no competing interests.

Additional information

Correspondence and requests for materials should be addressed to Y.P.